Electrochemistry of Gadolinium-Polyoxometalate Complexes in Concentrated Salt Solutions

Luke P. Soule*, Mary Louise E. Gucik, Jamin R. Pillars, Christian Arrington

Sandia National Laboratories, Albuquerque, New Mexico 87123

Polyoxometalates, Electrochemistry, Infrared Spectroscopy

ABSTRACT: Lanthanide-polyoxometalate complexes have been recently shown to possess unique magnetic, luminescent, and catalytic properties. While their electrochemical behavior has been explored in literature to some degree, the role of metallic species within the POM and nature and concentration of counter-cations in solutions has not been fully explained. The current work seeks to address this by studying the $Gd(OTf)_3$ – $[H_2W_{12}O_{40}]^{6-}$(MT) – $Si(W_{12}O_{40})^{-4}$ system in concentrated LiCl in N,N-dimethylformamide (DMF) using electrochemical and spectroscopic techniques. It was found that Gd^{3+} did not chemically bond to the POM species but interacted electrostatically through the O_t bonds of the MT POM but not Si based POM. Electrochemically, Gd^{3+} showed more reversible electrochemistry but was able to gain an additional electron in the presence of the MT^{-} species. The Si-POM did not show much electrochemical behavior in the presence of Li^+ and Gd^{3+} likely due to its non-interaction with both species, found using FTIR. The current work presents a step forward in the understanding of the role of metallic and cationic species in the electrochemical behavior of lanthanide-POM complexes.

Lanthanide-polyoxometalate complexes have recently shown unique magnetic, luminescent, and catalytic properties that can be readily exploited for new technological applications, such as infrared lasers, oxidative catalysis, energy storage, and single-molecule magnets.[1] As POMs are chemically rich molecules, numerous chemical interactions dictate their properties, such as the identity of the metal species in their structure and the nature of the counter-cation.[1-4] The current study seeks to clarify these chemical interactions by examining the electrochemical and spectroscopic behavior of $Gd(OTf)_3$, sodium metatungstate (SMT, $Na_6[H_2W_{12}O_{40}]$), tungstosilicic acid ($H_4[Si(W_{12}O_{40}]$), and concentrated LiCl in DMF. Concentrated LiCl was utilized to compare the electrochemistry of Gd^{3+}-MT^{3-} solutions to pure Gd^{3+}, which was found to require non-aqueous, solvent-in-salt like solutions when experiments are performed outside of an air-free environment. [5] It was found that Gd^{3+} and MT^{3-} weakly coordinated in solution without forming chemical bonds, as evidenced by UV-VIS. FTIR results found that concentrated Li^+ species shifted the O-H bending mode from asymmetric to symmetric, as well as disrupting the vibrational modes of C-H and C-N bonds in the DMF molecule. It was found that Gd^{3+} and MT^{3-} interacted via the terminal oxygen (O_t) of the POM as evidenced by suppression of the vibrational mode of the species. Additionally, the asymmetric stretching modes of the S-O bonds in the triflate anion were removed through the interaction of the two species, indicative of complex solution chemistry beyond Gd^{3+} and MT^{3-} interaction. Electrochemically, it was found that both Gd^{3+} and MT^{3-} species were not active in neat DMF but exhibited both reduction and oxidation peaks, and only reduction peaks for Gd and MT, respectively. The interaction of the two species resulted in an additional electron transfer during reduction for Gd^{3+} in the presence of MT^{3-} as well as shifting of oxidation peaks to a more negative potential. By modifying sweep rates, it was found that Gd^{3+} exhibited quasi-reversible reductive electrochemistry but irreversible oxidation and that MT^{3-} exhibited irreversible oxidation and reduction behavior likely due to the extreme distortion of the molecule in high ionic-strength solution. When the two were combined it was found that both exhibited irreversible electrochemistry in both oxidative and reductive regimes. For the $Si(W_{12}O_{40})^{4-}$ POM, virtually no electrochemistry occurred in the presence of Gd^{3+} and Li^+. FTIR of the solution also found little interaction between the POM and Gd^{3+} or Li^+. The reason for this behavior is not entirely clear. The current work provides fundamental insight into the role of cationic and metallic species in the electrochemical behavior of lanthanide-POM complexes.

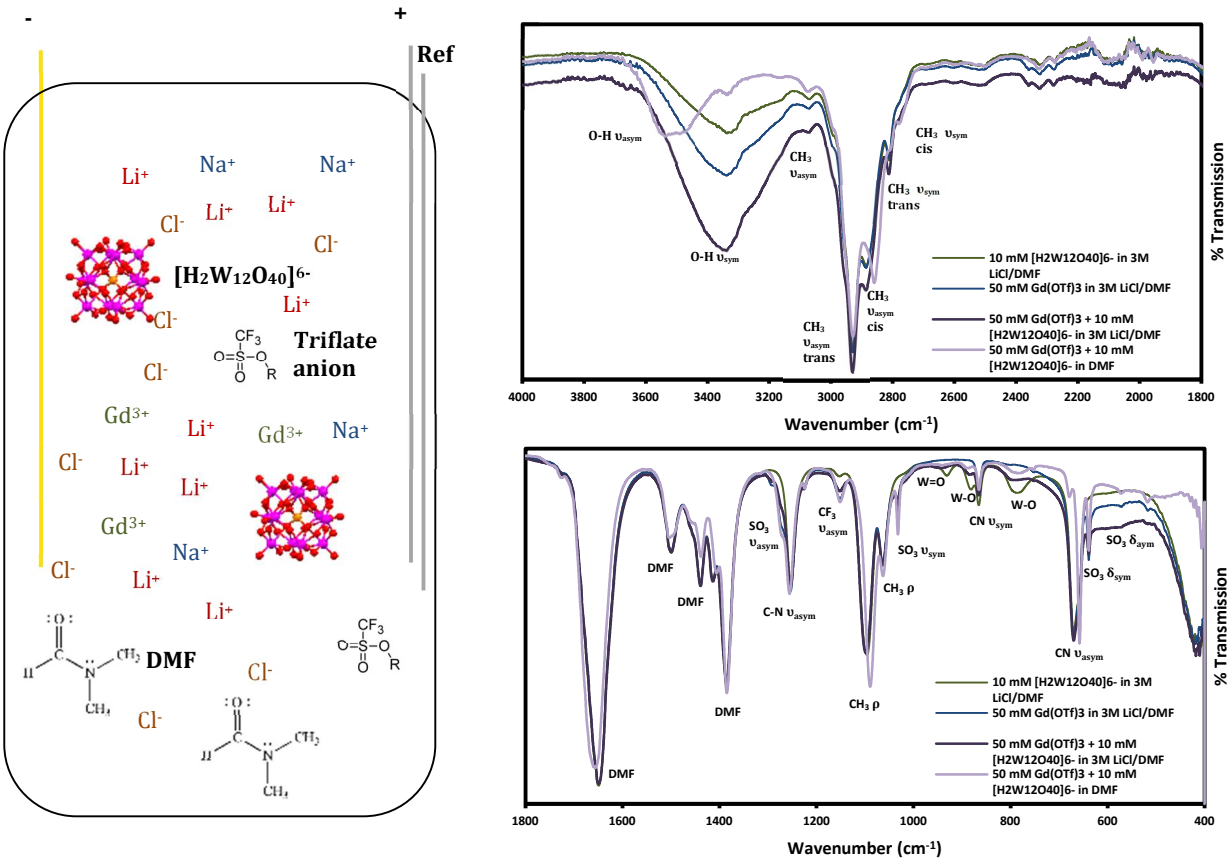

Figure 1. Schematic of electrochemical system (left), and FTIR spectrum of $Gd(OTf)_3$ and SMT with and without LiCl (right)

Figure 1 shows as schematic of the electrochemical system used in the current study. The solution is comprised of 30% salts by weight and 9.2% by volume, preventing the solution from being classified as 'solvent-in-salt'.[6] It should be noted that while the schematic depicts electrodes in close proximity, they are evenly spaced within the cell. The working electrode was an evaporate Au thin film on silicon. FTIR spectra of the system with and without LiCl is also depicted in Figure 1. Spectra of the neat DMF solvent with and without LiCl are depicted in Figure S1. Tabulated references for each peak is in Table S1. In terms of changes in the solvent when LiCl is introduced, the O-H stretching mode shifts from asymmetric stretching to symmetric stretching. It was found in literature that O-H peaks typically shift higher in wavenumber as more LiCl is added, indicative of increased interaction between chlorine ions and water.[7] Regarding LiCl in DMF, it was found that Li^+ bonds to the carbonyl oxygen on the DMF molecule, as evidenced by a shift in the bond at 660 cm^{-1} to 668 cm^{-1}, which was found in the current study.[8] Peak shifts involved with CH_3 stretching and rocking modes of the DMF molecule caused by LiCl solvation were found, indicative of either Cl^- or Li^+ interaction with the C-N-C side of the molecule. No interaction peaks or peak shifts were noticed with $Gd(OTf)_3$, or SMT addition, indicative of little interaction of the Gd^{3+} ion with both the MT^{6-} anion, the OTf^- ion, and with the LiCl/DMF solvent. It was found that Gd^{3+} is solvated by 8 DMF molecules by EXAFS.[9] The solvation of the molecule in concentrated LiCl DMF is unclear. In neat DMF solvent, Gd ions coordinate via the oxygen bond, which was found to be interact strongly with the Li^+ by FTIR, therefore the solvation of Gd^{3+} by DMF must be disrupted in some way in the current system. While the solvation of SMT in DMF is unclear, studies have found that lanthanide species, such as Gd^{3+}, readily form supramolecular networks with polyoxometalates that include 8 DMF molecules that readily exchange with the solution. [2] While not seen directly using FTIR, the solutions appear slightly opaque, which could indicate the formation of 3-D structures suspended in solution. Studies have found that the $W{=}O_t$ group of SMT binds to cationic species, which can been seen here as the intensity of the band greatly diminishes in the presence of Gd^{3+}.[4] As the intensity change in the W=O bond between the LiCl solution and the neat solvent do not differ greatly, it can be stated that Li^+ does not effect this bonding. The asymmetric SO_3 stretch from the triflate molecule nearly disappears in the presence of SMT molecules, also indicative of interaction of MT^{3-} with OTf^- anions. Due to their same charge, the nature of the interaction cannot be clarified.

UV-VIS was also performed to verify the findings of FTIR, shown in Figure S2. It was found that in the low wavelength regime, minimal changed occurred in spectra related to Gd-POM interaction besides a region between 300 and 340nm. In literature, it was found that for the UV-VIS spectra for POMs in DMF, peaks around 324 to 300nm is associated with the pπ to dπ transition from O_t to W.[10] Modifications in this region would make sense as cations in solution primarily interact with the terminal oxygen (O_t) of the POM, found both in literature and the current study using FTIR.[11] For other regions, no electron-ligand charge transfer is found (no new peaks arise from the interaction of MT^{3-} and Gd^{3+}), indicative of no strong complexing of the two species. In typical lanthanide-POM complexes, strong oxidizing species such as H_2O_2 or HNO_3 are required to chemically bond lanthanides within the POM complex.[12] As the current study does not utilize any such species, weak, electrostatic bonding between the POM and cations in solution is expected.

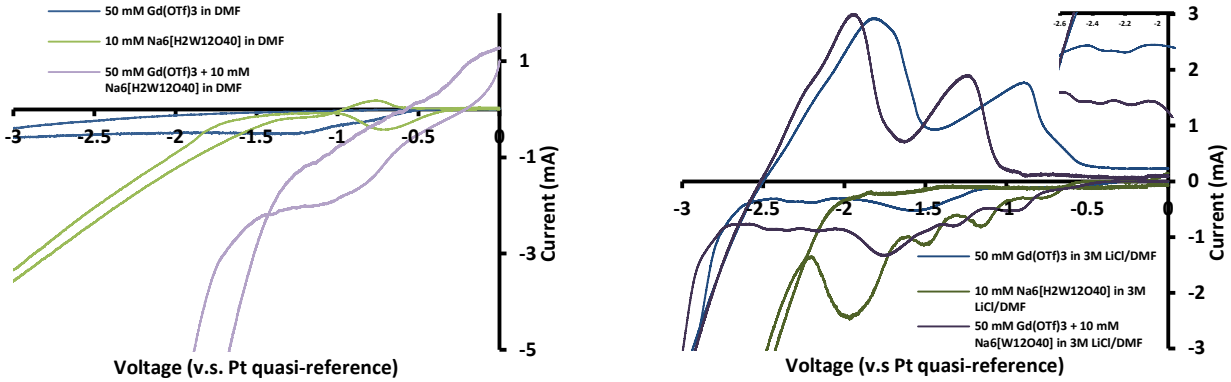

Figure 2. Cyclic voltammetry of $Gd(OTf)_3$ and SMT in neat solvent (left) and LiCl solutions (right)

To study the electrochemical behavior of the system, cyclic voltammetry was used. Figure 2 shows the cyclic voltammetry of $Gd(OTf)_3$ and SMT in neat DMF and concentrated solutions. Measurements were performed at 25 mV/s using a Pt quasi-reference electrode. In concentrated LiCl/DMF, the potential difference between Ag/AgCl and the Pt reference was -300mV. It was found that without LiCl, $Gd(OTf)_3$ in DMF exhibited a reduction plateau between -1.3 V (or -1V v.s. Ag/AgCl) and -3V. This behavior is similar to those found in literature where the plateau is attributed to mass-transfer limited proton diffusion.[5, 13] Additionally, a small slope is found between -0.5 and -1V. SMT exhibits a reduction peak around -0.7V and an oxidation peak around -0.8V. Studies have found LMT (lithium containing metatungstate) to undergo a 2 electron oxidation and reduction in DMF.[14] In current study, it was found that only a one electron transfer is possible without Li^+. The combination of SMT with Gd yields a broad slope starting at OCV, a small plateau between -1 and -1.5V, and a steep drop afterwards. No apparent reduction and oxidation peak appears for the combination of the two species. In the presence of LiCl, Gd^{3+} solutions appear to have one broad peak around -1.5V and a plateau between -2 and -2.7V. The plateau shows two small reduction peaks. On the reverse scan, a large oxidation peak appears around -1.8V and -0.8V with a small shoulder around -0.7V. In molten salt solutions, Gd^{3+} is reduced in a single electrochemical step around -2.3V (v.s. Ag/AgCl).[15] Inset is a zoomed in portion of the Gd plateau between -2 and -2.7V. The two reduction peaks are located at -2.2 and -2.3V for $Gd(OTf)_3$ and three at -2.2, -2.3, and -2.5V, indicative of a two and three electron transfer, respectively. For the SMT solution, four peaks at -0.8, -1.2, -1.5, and -2 can be seen. The first peak can be attributed to water break down while the other three can be attributed to 3 electron reduction steps.[14] When Gd^{3+} and MT^{3-} are combined, three peaks located at -1, -1.3, and -1.8V followed by the plateau between -2 and -2.5V seen with pure $Gd(OTf)_3$. Going off the shape of the peaks, each one matches that of the MT^{3-} species but shifted by 200mV. The plateau shows a three-electron transfer appose to a two. The oxidation reverse scan shows a shoulder at -2.2 and two peaks at -2, and -1.3V. These peaks match those of the Gd^{3+} peaks but are shifted by 300mV for the peak around -1.8V and 500mV for the peak around -0.8V. The shoulder around -0.7V diminishes and shifts to -0.9V. It was found that for actinide-POM complexes, reduction of the polyoxometalate aids in reduction of the actinide species by reducing the number of electrons required to change oxidation state, shifting from 1 to 0.72 electrons.[16] The current study has shown that MT^{3-} allows for an additional electron to be transferred during reduction as well as changing the oxidation behavior of the material.

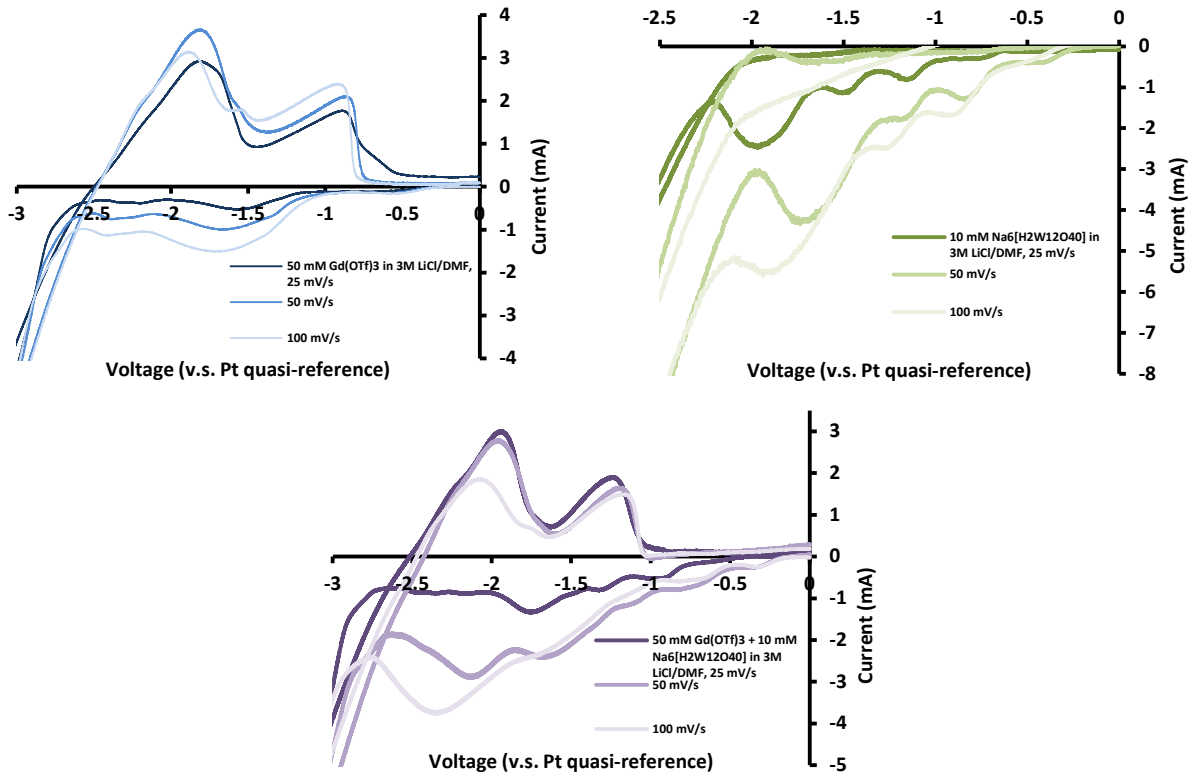

Figure 3. Cyclic Voltammetry at different scan rates for pure Gd^{3+} (top left), SMT (top right), and Gd^{3+} and SMT in 3M LiCl (bottom middle)

To further probe the electrochemical mechanisms and their kinetics, each redox active species was run separately at different scan rates and compared to the combined solution. For the $Gd(OTf)_3$ system, it was found that the plateau between -0.5 and -1V is not rate dependent, but all activity after -1.2V increases with scan rate. The peak around -1.7V increases at a faster rate than the multi-electron plateau between -2.1 and -2.5V. Assuming Gd^{3+}, the electron transfer at -1.7V is more kinetically limited than the subsequent electron transfers at -2.2 and -2.3V. For the oxidation scan, a shoulder peak is seen at -2.3V for 50 and 100 mV/s that is not seen at 25 mV/s, indicative of a fast electron transfer. The peak at -1.8V first increases in current as the scan rate increases, and at 100 mV/s the peak shifts to -1.9V. Additionally, at 100 mV/s, a new peak appears at -1.6V. The peak around -0.8V increases in current and then shifts to -0.9V at 100 mV/s. The shoulder peak at -0.7V disappears at higher scan rate. In kinetics studies in literature for Gd^{3+} deposited from molten salts, it was found that the reduction was quasi-reversible, or that the electron transfer rate was close to the rate of diffusion of Gd^{3+}.[17] Randles-Sevcik analysis was performed on the reduction peaks, found in Figure S3, where the first electron reduction in linear and the other two are linearly linear, indicative of a quasi-revisible, as found in literature.[18] For the oxidation peaks, due to their non-linear current v.s. scan rate behavior, the oxidation of Gd deposited is deemed irreversible and kinetically limited. For SMT, it was found that all reduction peaks shifted in potential in a non-linear fashion, shifting towards more positive potentials at 50 mV/s then to more negative potentials at 100 mV/s. All peaks exhibited quasi-revisibility from Randles-Sevcik analysis. In literature, it was found that all electron transfers were reversible as well with little peak shifting until 100 mV/s. As the current system using a concentrated LiCl solution (3M compared to 0.1M) and a different metal basis (W versus Mo), the two exhibit different electrochemical behavior.[14] Many recent studies have focused on the role of the counter ions in solutions, where it was found that electrostatic binding of alkali cations (Na and Li^+) interact strongly with the terminal oxo ligands of the polyoxometalate, which directly influences its electrochemical behavior.[3] Based on this reasoning, the strong interaction between Li^+ and terminal oxo ligands result in kinetic limitations for electron transfer and different potentials for these reactions. For the combined system, it was found that all reactions before -1.5V are irreversible as the 100 mV/s scan lay between the other two scan rates in terms of peak current. The peak around -1.7V before the 3-electron plateau between -2 and -2.5V, was found to show reversible behavior. Oxidation peaks showed a decrease in current with scan rate, indicative of a couple chemical-electrochemical reaction mechanism (C_rE_r).[18] In the combined system, the oxo ligands of the MT^- anion interact with both high charge Gd^{3+} ions as well as Li^+ resulting in even more distorted electrochemical behavior. However, as was found using UV-VIS no direct bonding between Gd^{3+} and MT^{3-} occurs, allowing for the two species to interchange electrons rather than directly bonding to one another.

The electrochemical behavior of Gd^{3+} complexed with the silicotungstic acid ($H_4[Si(W_{12}O_{40})]$) was also studied, shown

in Figure S4. It was found that little oxidation and reduction behavior occurred despite the increase solubility of the POM versus SMT. FTIR data, shown in the same figure, shows little to no complexing of the POM with species in solution while SMT shows some degree of complexing, as discussed previously. It has been found that silicotungstic acid shows two electron reduction and oxidation in 0.1M HCl.[19] The difference between the system found in literature and the current study is both the solvent (DMF versus water), and the ionic strength of the solution (H^+ has less interaction with the POM than Li^+) as well as the presence of Gd^{3+} might limit electrochemical reactions of the POM.

The current study examined the electrochemistry of gadolinium-POM complexes in concentrated LiCl-DMF solutions. It was found that Gd^{3+} and MT^{3-} electrostatically interacted rather than forming chemical bonds through the O_t group of the MT molecule. Electrochemically, it was found that Gd^{3+} exhibited more reversible electrochemistry but the interaction of the two species allowed for an additional electron transfer to occur in the regime of Gd electrodeposition. Si based POMs did not show electrochemical behavior in the presence of Gd^{3+} and showed virtually no electrostatic interaction between the POM and the cations in solution. The current work provides fundamental insight into the role of metallic and cationic species on the electrochemical behavior of lanthanide-POM complexes.

Experimental

Electrochemical experiments were carried out in a 100ml solution using a stainless-steel mesh anode, an Pt wire quasi-reference electrode, and a 500nm electron-beam evaporated Au coating on 1 in^2 Si substrates. The solution was agitated at a stir rate of 200 rpm during all measurements and heated at 80C. All chemicals were purchased through Sigma Aldrich. Electrochemical measurements were performed on a Voltalab universal pulse dynamic-EIS voltammetry PGZ402 instrument. FTIR was acquired in attenuated-reflection mode using a Nicolet iS20 from Thermo Fisher.

The manuscript was written through contributions of all authors. All authors have given approval to the final version of the manuscript.

Funding Sources

The authors gratefully acknowledge funding from U.S. Department of Energy, Laboratory Directed Research and Development program project #232149. Research was performed at Sandia National Laboratories, a multi-mission laboratory managed and operated by National technology and Engineering Solutions of Sandia LLC, a wholly owned subsidiary of Honeywell International Inc., for the U.S. Department of Energy's National Nuclear Security Administration under Contract No. DE-NA000352

ASSOCIATED CONTENT

Table S1 references and FTIR band assignments, Figure S1 FTIR bands of neat DMF with and with LiCl, Figure S2. UV-VIS spectra of electrolytes, Figure S3. R-S analysis of POM and Gd species, S4. Electrochemical behavior of Silicotungstate POM in LiCl/DMF. This material is available free of charge via the Internet at http://pubs.acs.org.

AUTHOR INFORMATION

Corresponding Author

*lpsoule@sandia.gov

Author Contributions

REFERENCES

(1) Granadeiro, C. M.; Julião, D.; Ribeiro, S. O.; Cunha-Silva, L.; Balula, S. S. Recent advances in lanthanide-coordinated polyoxometalates: from structural overview to functional materials. *Coordination Chemistry Reviews* **2023**, *476*, 214914. DOI: https://doi.org/10.1016/j.ccr.2022.214914.

(2) Tang, Q.; Liu, S.-X.; Liang, D.-D.; Ma, F.-J.; Ren, G.-J.; Wei, F.; Yang, Y.; Li, C.-C. Lanthanide-organic complexes based on polyoxometalates: Solvent effect on the luminescence properties. *Journal of Solid State Chemistry* **2012**, *190*, 85-91. DOI: https://doi.org/10.1016/j.jssc.2012.02.006.

(3) Misra, A.; Kozma, K.; Streb, C.; Nyman, M. Beyond Charge Balance: Counter-Cations in Polyoxometalate Chemistry. *Angewandte Chemie International Edition* **2020**, *59* (2), 596-612, https://doi.org/10.1002/anie.201905600. DOI: https://doi.org/10.1002/anie.201905600 (acccessed 2023/07/10).

(4) Primera-Pedrozo, O. M.; Tan, S.; Zhang, D.; O'Callahan, B. T.; Cao, W.; Baxter, E. T.; Wang, X.-B.; El-Khoury, P. Z.; Prabhakaran, V.; Glezakou, V.-A.; et al. Influence of surface and intermolecular interactions on the properties of supported polyoxometalates. *Nanoscale* **2023**, *15* (12), 5786-5797, 10.1039/D2NR06148A. DOI: 10.1039/D2NR06148A.

(5) Gucik, M. L.; Pillars, J. R.; Strange, L.; Arrington, C. L.; Jau, Y.-Y. *Electrodeposition of gadolinium metal from organic solvents*; Sandia National Lab.(SNL-NM), Albuquerque, NM (United States), 2020.

(6) Suo, L.; Hu, Y.-S.; Li, H.; Armand, M.; Chen, L. A new class of Solvent-in-Salt electrolyte for high-energy rechargeable metallic lithium batteries. *Nature Communications* **2013**, *4* (1), 1481. DOI: 10.1038/ncomms2513.

(7) Roget, S. A.; Carter-Fenk, K. A.; Fayer, M. D. Water Dynamics and Structure of Highly Concentrated LiCl Solutions Investigated Using Ultrafast Infrared Spectroscopy. *Journal of the American Chemical Society* **2022**, *144* (9), 4233-4243. DOI: 10.1021/jacs.2c00616.

(8) Lassigne, C.; Baine, P. Solvation studies of lithium salts in dimethylformamide. *The Journal of Physical Chemistry* **1971**, *75* (20), 3188-3190.

(9) Fuchs, A.; Lundberg, D.; Warmińska, D.; Persson, I. On the Structure and Volumetric Properties of Solvated

Lanthanoid(III) Ions in Amide Solutions. *The Journal of Physical Chemistry B* **2013**, *117* (28), 8502-8511. DOI: 10.1021/jp310111j.

(10) Li, H.; Pan, H.; Fan, Y.; Bai, Y.; Dang, D. Syntheses, crystal structures, and properties of four polyoxometalate-based metal–organic frameworks based on Ag(I) and 4,4′-dipyridine-N,N′-dioxide. *Polyoxometalates* **2022**, *1* (2), 9140007. DOI: 10.26599/POM.2022.9140007.

(11) Gunaratne, K. D. D.; Johnson, G. E.; Andersen, A.; Du, D.; Zhang, W.; Prabhakaran, V.; Lin, Y.; Laskin, J. Controlling the Charge State and Redox Properties of Supported Polyoxometalates via Soft Landing of Mass-Selected Ions. *The Journal of Physical Chemistry C* **2014**, *118* (48), 27611-27622. DOI: 10.1021/jp505050m.

(12) Liang, Z.; Wu, H.; Singh, V.; Qiao, Y.; Li, M.; Ma, P.; Niu, J.; Wang, J. Assembly of Lanthanide-Containing Polyoxotantalate Clusters with Efficient Photoluminescence Properties. *Inorganic Chemistry* **2019**, *58* (19), 13030-13036. DOI: 10.1021/acs.inorgchem.9b01952. Zhang, H.; Li, A.; Li, K.; Wang, Z.; Xu, X.; Wang, Y.; Sheridan, M. V.; Hu, H.-S.; Xu, C.; Alekseev, E. V.; et al. Ultrafiltration separation of Am(VI)-polyoxometalate from lanthanides. *Nature* **2023**, *616* (7957), 482-487. DOI: 10.1038/s41586-023-05840-z.

(13) Sides, W. D.; Hassani, E.; Pappas, D. P.; Hu, Y.; Oh, T.-S.; Huang, Q. Grain growth and superconductivity of rhenium electrodeposited from water-in-salt electrolytes. *Journal of Applied Physics* **2020**, *127* (8).

(14) Cao, Y.; Chen, J.-J. J.; Barteau, M. A. Systematic approaches to improving the performance of polyoxometalates in non-aqueous redox flow batteries. *Journal of Energy Chemistry* **2020**, *50*, 115-124. DOI: https://doi.org/10.1016/j.jechem.2020.03.009.

(15) Bermejo, M. R.; Gómez, J.; Medina, J.; Martínez, A. M.; Castrillejo, Y. The electrochemistry of gadolinium in the eutectic LiCl–KCl on W and Al electrodes. *Journal of Electroanalytical Chemistry* **2006**, *588* (2), 253-266. DOI: https://doi.org/10.1016/j.jelechem.2005.12.031.

(16) Chiang, M.-H.; Soderholm, L.; Antonio, Mark R. Redox Chemistry of Actinide Ions in Wells−Dawson Heteropolyoxoanion Complexes. *European Journal of Inorganic Chemistry* **2003**, *2003* (16), 2929-2936, https://doi.org/10.1002/ejic.200300225. DOI: https://doi.org/10.1002/ejic.200300225 (acccessed 2023/07/06).

(17) Tang, H.; Pesic, B. Electrochemistry and Electrocrystallization of Gadolinium on Mo Substrate in LiCl–KCl Eutectic Salts. *Journal of The Electrochemical Society* **2014**, *161* (9), D429. DOI: 10.1149/2.0371409jes.

(18) Elgrishi, N.; Rountree, K. J.; McCarthy, B. D.; Rountree, E. S.; Eisenhart, T. T.; Dempsey, J. L. A practical beginner's guide to cyclic voltammetry. *Journal of chemical education* **2018**, *95* (2), 197-206.

(19) Cox, J. A.; Wolkiewicz, A. M.; Kulesza, P. J. Solid-state electrochemistry of silicotungstic acid immobilized by sol-gel chemistry. *Journal of Solid State Electrochemistry* **1998**, *2* (4), 247-252. DOI: 10.1007/s100080050095.

Electrochemistry of Gadolinium-Polyoxometalate Complexes in Concentrated Salt Solutions

Luke P. Soule*, Mary Louise E. Gucik, Jamin R. Pillars, Christian Arrington

Sandia National Laboratories, Albuquerque, New Mexico 87123

Polyoxometalates, Electrochemistry, Infrared Spectroscopy

Supplementary Information

Measure Wavenumber (cm^{-1})	Theoretical Wavenumber (cm^{-1})	Bond
3548	3010-4000	O-H, asym stretch[20]
3326	3010-4000	O-H, sym stretch[20]
3070	3143	CH_3 asym stretch, DMF[21]
2996	2992	CH_3 asym stretch, trans, DMF[21]
2928	2930	CH_3 asym stretch, cis, DMF[21]
2883	N/A	LiCl-DMF
2857	2860	CH_3 sym stretch, trans, DMF[21]
2811	2810	CH_3 sym stretch, cis, DMF[21]
2804	2810	CH_3 sym stretch, cis, DMF[21]
1955	N/A	N/A
1706	1730	DMF[21]
1652	1677	DMF[21]
1648	N/A	LiCl-DMF
1501	1507	DMF[21]
1438	1440	DMF[21]
1400	1397	DMF[21]
1385	1385	DMF[21]
1286	N/A	$Gd(OTf)_3$ – LiCl - DMF

1271	1270	Asym stretch, SO_3, OTf^- [22]
1253	1255	CN asym stretch, DMF[21]
1240	1247	Sym stretch, CF_3, OTf^- [22]
1094	N/A	LiCl-DMF
1088	1093	CH_3 rock, DMF[21]
1063	1063	CH_3 rock, DMF[21]
1031	1032	Sym stretch, SO_3, OTf^- [22]
971	981	Asym stretch, Si-O[23]
930	930	W=O, $Na_6[H_2W_{12}O_{44}]$[24]
921	928	Asym stretch W-O-W[1]
881	881	W-O, $Na_6[H_2W_{12}O_{44}]$[24]
865	863	CN sym stretch, DMF[21]
802	804	Si POM[23]
784	785	W-O, $Na_6[H_2W_{12}O_{44}]$[24]
751	751	CF_3 sym deformation, OTf^- [22]
668	N/A	LiCl-DMF
657	658	NCO bend + CN stretch, CN asym stretch, DMF[21]
638	637	SO_3 sym deformation, OTf^- [22]
571	572	CF_3 asym deformation, OTf^- [22]
507	510	SO_3 asym deformation, OTf^- [22]
407	403	CNC scissor, DMF[21]

Table S1. FTIR peak assignments

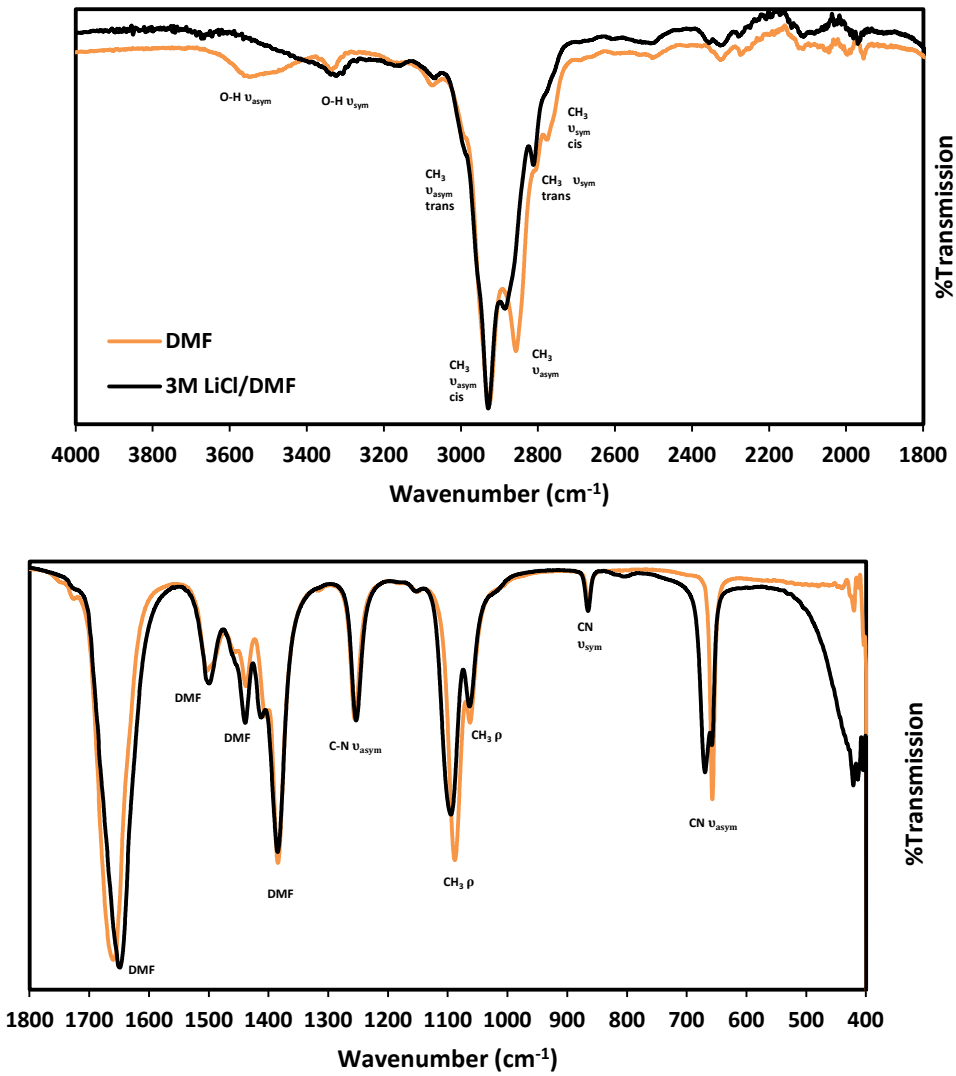

Figure S1. FTIR spectra, 3M LiCl in DMF and neat DMF

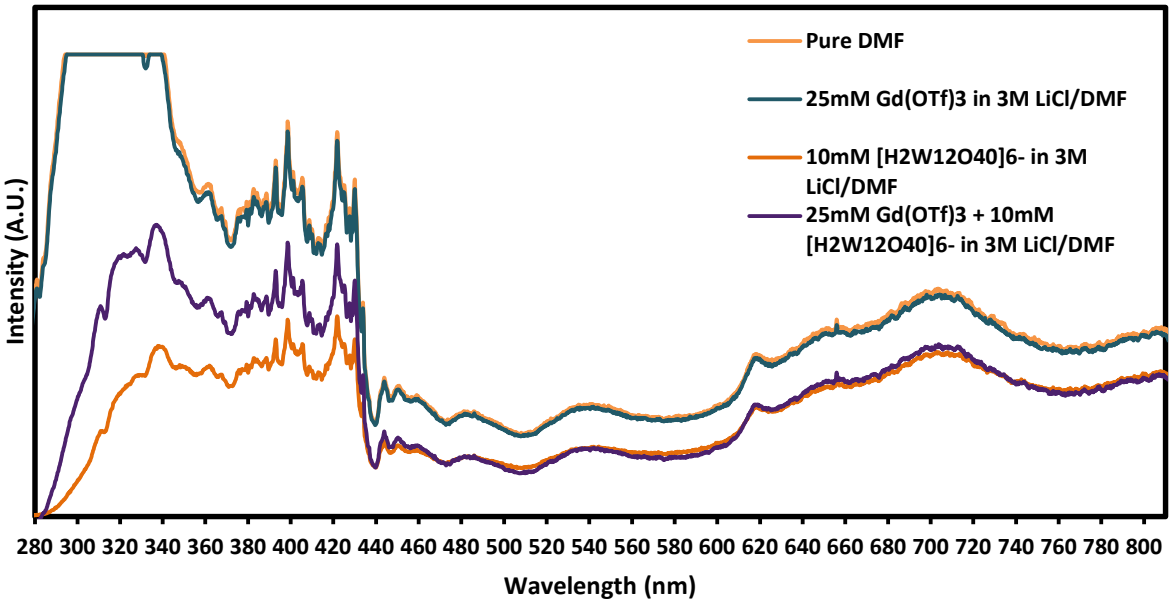

Figure S2. UV-VIS spectra of all species

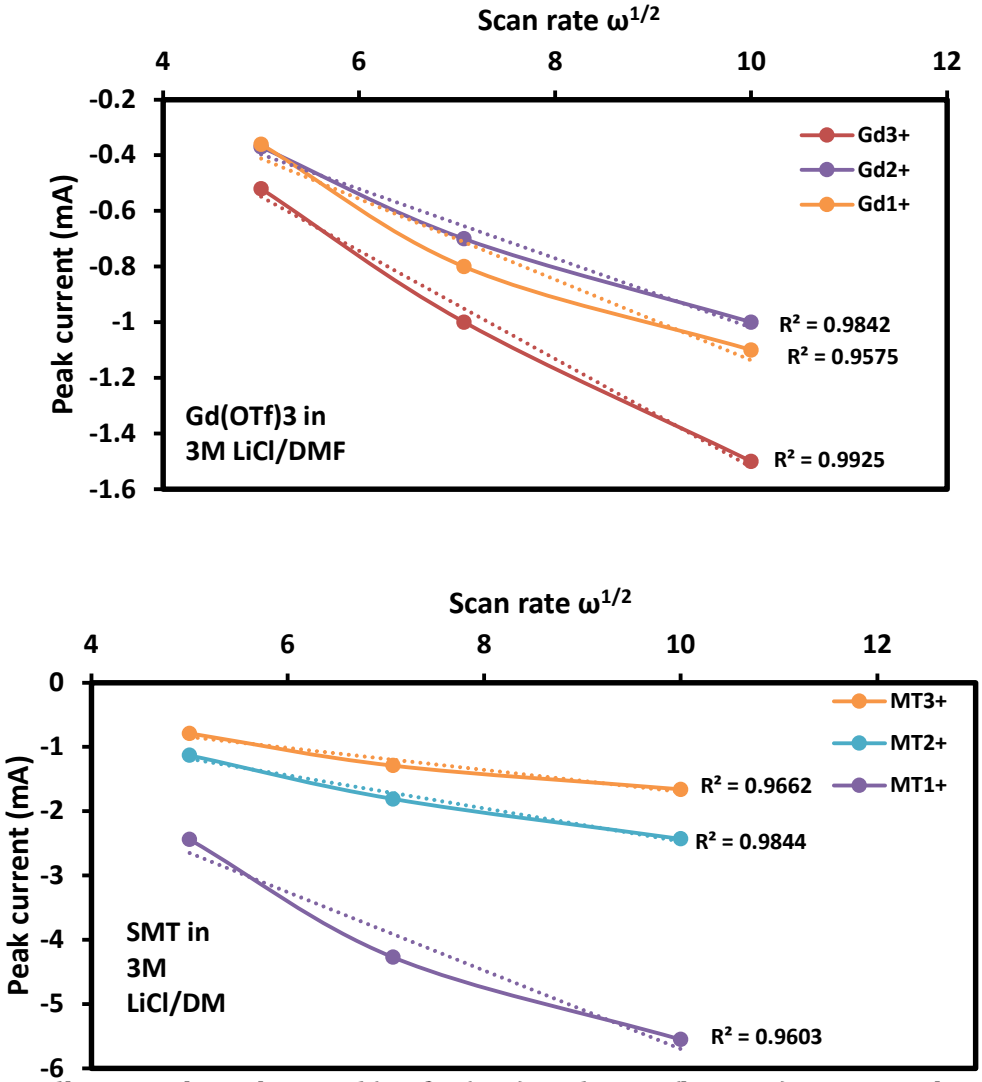

Figure S3. Randles-Sevcik analysis $Gd(OTf)_3$ (top) and SMT (bottom) in 3M LiCl, reductive scan

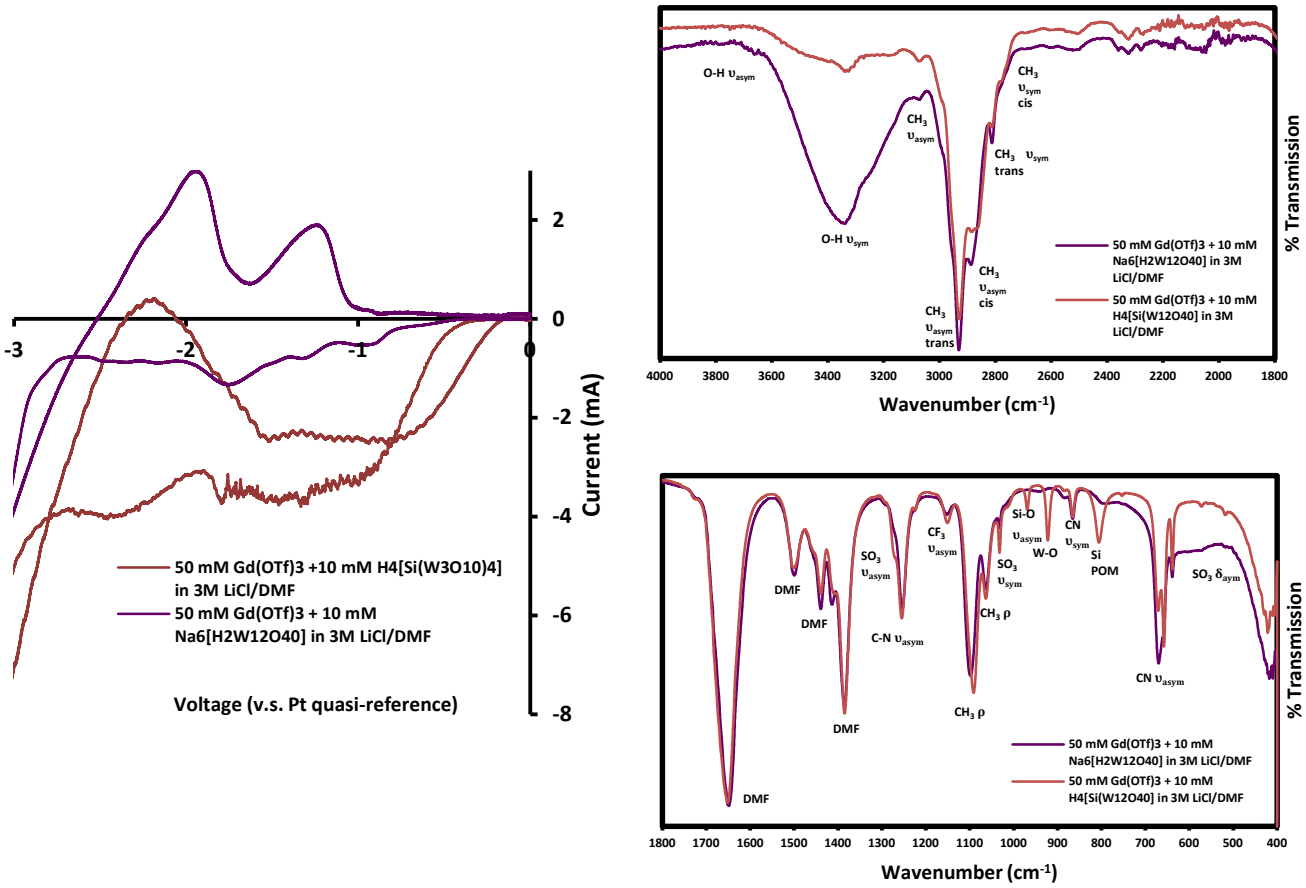

Figure S4. CV data of Silicotungstate POM with Gd in Solvent-in-Salt, left, and FTIR spectra (right)

References

(1) Granadeiro, C. M.; Julião, D.; Ribeiro, S. O.; Cunha-Silva, L.; Balula, S. S. Recent advances in lanthanide-coordinated polyoxometalates: from structural overview to functional materials. *Coordination Chemistry Reviews* **2023**, *476*, 214914. DOI: https://doi.org/10.1016/j.ccr.2022.214914.

(2) Tang, Q.; Liu, S.-X.; Liang, D.-D.; Ma, F.-J.; Ren, G.-J.; Wei, F.; Yang, Y.; Li, C.-C. Lanthanide-organic complexes based on polyoxometalates: Solvent effect on the luminescence properties. *Journal of Solid State Chemistry* **2012**, *190*, 85-91. DOI: https://doi.org/10.1016/j.jssc.2012.02.006.

(3) Misra, A.; Kozma, K.; Streb, C.; Nyman, M. Beyond Charge Balance: Counter-Cations in Polyoxometalate Chemistry. *Angewandte Chemie International Edition* **2020**, *59* (2), 596-612, https://doi.org/10.1002/anie.201905600. DOI: https://doi.org/10.1002/anie.201905600 (acccessed 2023/07/10).

(4) Primera-Pedrozo, O. M.; Tan, S.; Zhang, D.; O'Callahan, B. T.; Cao, W.; Baxter, E. T.; Wang, X.-B.; El-Khoury, P. Z.; Prabhakaran, V.; Glezakou, V.-A.; et al. Influence of surface and intermolecular interactions on the properties of supported polyoxometalates. *Nanoscale* **2023**, *15* (12), 5786-5797, 10.1039/D2NR06148A. DOI: 10.1039/D2NR06148A.

(5) Gucik, M. L.; Pillars, J. R.; Strange, L.; Arrington, C. L.; Jau, Y.-Y. *Electrodeposition of gadolinium metal from organic solvents*; Sandia National Lab.(SNL-NM), Albuquerque, NM (United States), 2020.
(6) Suo, L.; Hu, Y.-S.; Li, H.; Armand, M.; Chen, L. A new class of Solvent-in-Salt electrolyte for high-energy rechargeable metallic lithium batteries. *Nature Communications* **2013**, *4* (1), 1481. DOI: 10.1038/ncomms2513.
(7) Roget, S. A.; Carter-Fenk, K. A.; Fayer, M. D. Water Dynamics and Structure of Highly Concentrated LiCl Solutions Investigated Using Ultrafast Infrared Spectroscopy. *Journal of the American Chemical Society* **2022**, *144* (9), 4233-4243. DOI: 10.1021/jacs.2c00616.
(8) Lassigne, C.; Baine, P. Solvation studies of lithium salts in dimethylformamide. *The Journal of Physical Chemistry* **1971**, *75* (20), 3188-3190.
(9) Fuchs, A.; Lundberg, D.; Warmińska, D.; Persson, I. On the Structure and Volumetric Properties of Solvated Lanthanoid(III) Ions in Amide Solutions. *The Journal of Physical Chemistry B* **2013**, *117* (28), 8502-8511. DOI: 10.1021/jp310111j.
(10) Li, H.; Pan, H.; Fan, Y.; Bai, Y.; Dang, D. Syntheses, crystal structures, and properties of four polyoxometalate-based metal–organic frameworks based on Ag(I) and 4,4′-dipyridine-N,N′-dioxide. *Polyoxometalates* **2022**, *1* (2), 9140007. DOI: 10.26599/POM.2022.9140007.
(11) Gunaratne, K. D. D.; Johnson, G. E.; Andersen, A.; Du, D.; Zhang, W.; Prabhakaran, V.; Lin, Y.; Laskin, J. Controlling the Charge State and Redox Properties of Supported Polyoxometalates via Soft Landing of Mass-Selected Ions. *The Journal of Physical Chemistry C* **2014**, *118* (48), 27611-27622. DOI: 10.1021/jp505050m.
(12) Liang, Z.; Wu, H.; Singh, V.; Qiao, Y.; Li, M.; Ma, P.; Niu, J.; Wang, J. Assembly of Lanthanide-Containing Polyoxotantalate Clusters with Efficient Photoluminescence Properties. *Inorganic Chemistry* **2019**, *58* (19), 13030-13036. DOI: 10.1021/acs.inorgchem.9b01952. Zhang, H.; Li, A.; Li, K.; Wang, Z.; Xu, X.; Wang, Y.; Sheridan, M. V.; Hu, H.-S.; Xu, C.; Alekseev, E. V.; et al. Ultrafiltration separation of Am(VI)-polyoxometalate from lanthanides. *Nature* **2023**, *616* (7957), 482-487. DOI: 10.1038/s41586-023-05840-z.
(13) Sides, W. D.; Hassani, E.; Pappas, D. P.; Hu, Y.; Oh, T.-S.; Huang, Q. Grain growth and superconductivity of rhenium electrodeposited from water-in-salt electrolytes. *Journal of Applied Physics* **2020**, *127* (8).
(14) Cao, Y.; Chen, J.-J. J.; Barteau, M. A. Systematic approaches to improving the performance of polyoxometalates in non-aqueous redox flow batteries. *Journal of Energy Chemistry* **2020**, *50*, 115-124. DOI: https://doi.org/10.1016/j.jechem.2020.03.009 .
(15) Bermejo, M. R.; Gómez, J.; Medina, J.; Martínez, A. M.; Castrillejo, Y. The electrochemistry of gadolinium in the eutectic LiCl–KCl on W and Al electrodes. *Journal of Electroanalytical Chemistry* **2006**, *588* (2), 253-266. DOI: https://doi.org/10.1016/j.jelechem.2005.12.031.
(16) Chiang, M.-H.; Soderholm, L.; Antonio, Mark R. Redox Chemistry of Actinide Ions in Wells−Dawson Heteropolyoxoanion Complexes. *European Journal of Inorganic Chemistry* **2003**, *2003* (16), 2929-2936, https://doi.org/10.1002/ejic.200300225. DOI: https://doi.org/10.1002/ejic.200300225 (acccessed 2023/07/06).
(17) Tang, H.; Pesic, B. Electrochemistry and Electrocrystallization of Gadolinium on Mo Substrate in LiCl–KCl Eutectic Salts. *Journal of The Electrochemical Society* **2014**, *161* (9), D429. DOI: 10.1149/2.0371409jes.

(18) Elgrishi, N.; Rountree, K. J.; McCarthy, B. D.; Rountree, E. S.; Eisenhart, T. T.; Dempsey, J. L. A practical beginner's guide to cyclic voltammetry. *Journal of chemical education* **2018**, *95* (2), 197-206.
(19) Cox, J. A.; Wolkiewicz, A. M.; Kulesza, P. J. Solid-state electrochemistry of silicotungstic acid immobilized by sol-gel chemistry. *Journal of Solid State Electrochemistry* **1998**, *2* (4), 247-252. DOI: 10.1007/s100080050095.
(20) Palencia, M. Functional transformation of Fourier-transform mid-infrared spectrum for improving spectral specificity by simple algorithm based on wavelet-like functions. *Journal of Advanced Research* **2018**, *14*, 53-62. DOI: https://doi.org/10.1016/j.jare.2018.05.009.
(21) Shastri, A.; Das, A. K.; Krishnakumar, S.; Singh, P. J.; Raja Sekhar, B. N. Spectroscopy of N,N-dimethylformamide in the VUV and IR regions: Experimental and computational studies. *The Journal of Chemical Physics* **2017**, *147* (22), 224305. DOI: 10.1063/1.5006126 (acccessed 7/5/2023).
(22) Johnston, D. H.; Shriver, D. F. Vibrational study of the trifluoromethanesulfonate anion: unambiguous assignment of the asymmetric stretching modes. *Inorganic Chemistry* **1993**, *32* (6), 1045-1047. DOI: 10.1021/ic00058a050.
(23) Zhang, Q.; Yang, B.; Tian, Y.; Yang, X.; Yu, R.; Wang, J.; Deng, T.; Zhang, Y. Fabrication of silicotungstic acid immobilized on Ce-based MOF and embedded in Zr-based MOF matrix for green fatty acid esterification. **2022**, *11* (1), 184-194. DOI: doi:10.1515/gps-2022-0021 (acccessed 2023-07-06).
(24) Hunyadi, D.; Sajó, I.; Szilágyi, I. M. Structure and thermal decomposition of ammonium metatungstate. *Journal of Thermal Analysis and Calorimetry* **2014**, *116* (1), 329-337. DOI: 10.1007/s10973-013-3586-1.